CHEMISTRY OF MATERIALS

Article

pubs.acs.org/cm

Carbazole/Sulfone Hybrid D-π-A-Structured Bipolar Fluorophores for High-Efficiency Blue-Violet Electroluminescence

Jun Ye,[†,‡,∥] Zhan Chen,[†,∥] Man-Keung Fung,[‡] Caijun Zheng,[†] Xuemei Ou,[†] Xiaohong Zhang,*[,†] Yi Yuan,[‡,§] and Chun-Sing Lee*[,‡]

[†]Nano-organic Photoelectronic Laboratory and Key Laboratory of Photochemical Conversion and Optoelectronic Materials, Technical Institute of Physics and Chemistry, Chinese Academy of Sciences, Beijing 100190, P.R. China

[‡]Center of Super-Diamond and Advanced Films (COSDAF) and Department of Physics and Materials Sciences, City University of Hong Kong, Hong Kong SAR, P.R. China

[§]Department of Chemistry, Shantou University, Guangdong 515063, P.R. China

Supporting Information

ABSTRACT: Based on a D-π-A structural strategy incorporating carbazole as a mild electron-donor and sulfone as an electron-acceptor with a π-conjugation-breaking feature, two novel blue-violet emitting materials (CzS1 and CzS2) were successfully designed and synthesized. The two compounds exhibit high-efficiency fluorescent emissions of intramolecular charge-transfer transition type, with impressively high quantum yields in both solution and film states. CIE_y below 0.06 and excellent current/power efficiencies up to 1.89 cd A^{-1}/1.58 lm W^{-1} were achieved with their corresponding nondoped devices. These performances currently represent the best results for OLEDs with CIE_y < 0.06. Moreover, single-carrier devices were also fabricated to demonstrate the bipolar characteristics as well as to understand the different electroluminescence performance of the two fluorophores.

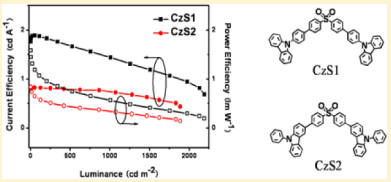

KEYWORDS: *blue-violet electroluminescence, carbazole, sulfone, bipolar fluorophor*

INTRODUCTION

Blue-violet/violet light-emitting materials are of great significance for their unique applications in flat-panel displays[1] and high-density information storage.[2] Especially in full-color displays, the short-wavelength emission can not only serve as an excitation source for emission over the whole visible range and white light emission, but also is a key component for effectively reducing the power consumption of the display.[3] Therefore, the development of high-efficiency blue-violet to violet emitting materials and devices are important for the rapidly developing organic light-emitting device (OLED) technology.

However, so far, the reports of efficient OLEDs with their color coordinates in the Commission Internationale de L'Eclairage (CIE) chromaticity diagram beyond the standard blue (CIE coordinates of 0.15, 0.06), are still rare.[4] Many efficient emitters, such as anthracene,[5] fluorene,[6] styrylarylene[7] and pyrene derivatives,[8] and so forth, are based on molecular structures of large π conjugation which can give highly emissive π−π* transition states upon excitation. However, for realizing blue-violet or violet emission the π conjugation of organic molecules must be strictly confined. This will then either cause co-instantaneous decrease of fluorescent quantum yield and charge-transporting ability,[9] or to some extent increase the synthetic difficulty when large molecular weight and/or bulky structure are usually required for good thermal and morphological stability. Very recently, donor-π-acceptor (D-π-A) type fluorophores have attracted much attention because they not only show high fluorescent quantum yields owing to the effective radiative decay of their excited intramolecular charge-transfer (ICT) state but also possess impressive bipolar charge-transporting properties for their constituting hole- and electron-transporting moieties.[10] As a result, the use of D-π-A type fluorophores can effectively simplify the device configurations[10a,d,e,g] and tremendously enhance the electroluminescence (EL) efficiencies of OLEDs.[10] However, except for the enlarged π conjugation, the ICT trend in such molecules indeed could also lead to remarkable fluorescence red shifts.[10c] Basing on a central A group of phosphine oxide that can break the local π conjugation, Liu et al. recently developed a series of efficient deep-blue emitters which show electroluminescence CIE coordinates around (0.15, 0.10).[10j] Whereas room for further blue-shifting the emission still remains because the strong electron-donating *N*-phenylnaphthalen-1-amine group (with relatively low oxidation potentials)[10j] and long π bridges between the D and A units (3 to 4 benzene rings) were used in these emitters. Once replaced by other less electron-rich donors and shorter π bridges, respectively, to limit the ICT trend and the molecular conjugation, the light emission can be further adjusted to shorter wavelength. Moss et al. systematically studied the photophysics of a series of electron-accepting dibenzothiophene S,S-dioxide (DBTO)-based fluorophores

Received: March 22, 2013
Revised: June 9, 2013

   dx.doi.org/10.1021/cm400945h | *Chem. Mater.* XXXX, XXX, XXX−XXX

Scheme 1. Synthesis of CzS1 and CzS2

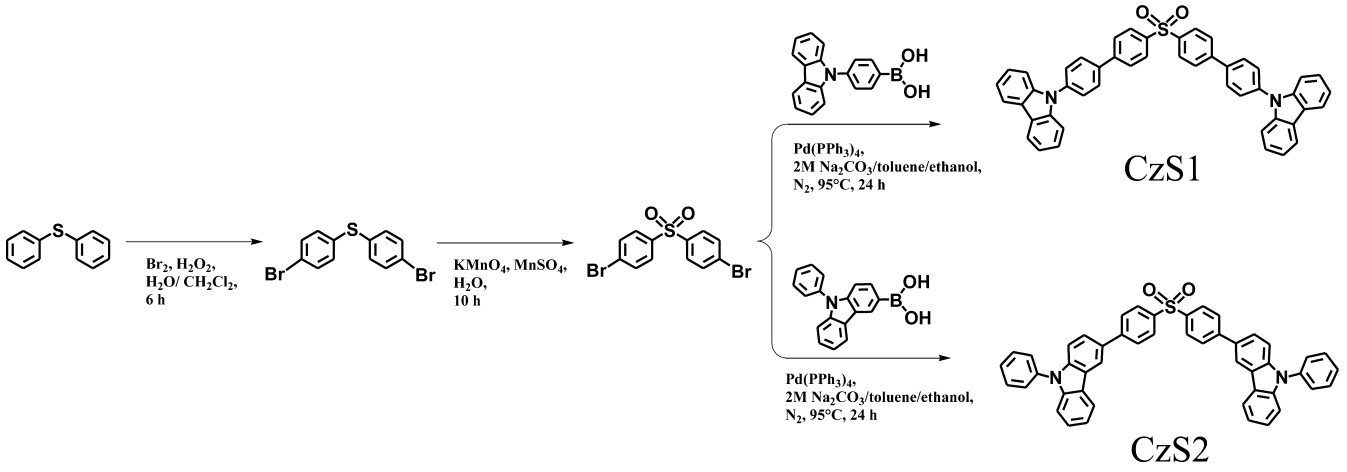

which are modified with different kinds of D units.[11] Among them, the carbazole/DBTO-connected fluorophores exhibit blue to violet (450 to 408 nm) fluorescence in toluene solution. Their fluorescent quantum yields are yet either moderate (0.58) or even low (0.25). It is also noticeable that substantial conjugation exists across the DBTO unit, still leaving the chance for further blue-shifting the emission. Thereby, the key point for designing high-efficiency blue-violet to violet electroluminescence materials is to suitably control the π-conjugation enlargement and the ICT trend inside the molecules.

Herein, we utilized a carbazole/sulfone hybrid design strategy to obtain two novel efficient blue-violet fluorophores, di(4-(4-(carbazol-9-yl)phenyl)phenyl)sulfone (**CzS1**) and di(4-(9-phenylcarbazol-3-yl)phenyl)sulfone (**CzS2**) (Scheme 1). The widely used hole-transporting moiety, carbazole, was selected as the electron-donor (D) for its relatively mild electron-donating ability as compared to other arylamines.[10c] These D-π-A type molecules could thus have relatively weak ICT trends, which is beneficial for generating short-wavelength emissions. Besides, the sulfone group was chosen as the electron-acceptor (A) for its excellent electron injection/transporting properties.[10a,12] More importantly, the sulfone, as linked to two freely rotatable benzene rings in this work, can also serve as a π-conjugation breaker because of its tetrahedral electronic conformation which could effectively confine the π-conjugation of the molecules. Finally, these compounds were designed to be bulky to enhance their morphological and thermal stability by using a symmetrical D-π-A-π-D structure. Bipolar charge-transporting characteristics of CzS1 and CzS2 were demonstrated with single-carrier type devices. Nondoped OLEDs based on the two novel fluorophores show blue-violet light emissions with $CIE_{x,y}$ of (0.157, 0.055) and (0.157, 0.044), respectively. The CzS1-based device exhibited excellent EL performance with high external quantum efficiency (EQE) of 4.2%, current efficiency (CE) of 1.89 cd A^{-1}, and power efficiency (PE) of 1.58 lm W^{-1}. Performances of the devices are among the best of OLEDs with CIE_y below 0.06. In particular, to the best of our knowledge, the CE and PE obtained here have reached the highest values of reported blue-violet/violet OLEDs with CIE_y below 0.06.

EXPERIMENTAL SECTION

General Procedures. ^1H and ^{13}C NMR spectra were measured with a Varian Gemini-400 Varian spectrometer. Mass spectra were recorded on a Finnigan 4021C GC-MS spectrometer. Differential scanning calorimetry (DSC) was performed using a Perkin-Elmer Pyris DSC 6 instrument operated at a heating rate of 10 °C min^{-1} in a nitrogen atmosphere. The glass transition temperature (T_g) was determined from the second heating scan. Thermogravimetric analysis (TGA) was undertaken using a TA SDT Q600 instrument. The thermal stability of the samples under a nitrogen atmosphere was determined by measuring their weight losses while heating at a rate of 20 °C min^{-1}. The absorption and emission spectra were recorded on a Hitachi U-3010 UV−vis spectrophotometer and a Hitachi F-4500 fluorescence spectrophotometer, respectively. The film photoluminescence quantum yield was measured by the integrating sphere method, and the emission decay profile was measured with an Edinburgh F900 fluorescence spectrophotometer. Cyclic voltammetry was performed with a CHI600A analyzer with the scan rate of 100 mV s^{-1} at room temperature. The electrolytic cell was a conventional three-electrode cell in which a glassy carbon working electrode, a Pt wise auxiliary electrode, and an aqueous saturated calomel electrode (SCE) as the reference electrode were employed. Tetra-*n*-butylammoniumhexafluorophosphate ($TBAPF_6$, 0.10 M) was used as the supporting electrolyte and CH_2Cl_2 as the solvent, respectively. The ferrocene/ferrocenium couple was used as the internal standard.

Synthesis. All solvents and materials were used as received from commercial suppliers without further purification. Synthetic routes of the two compounds are outlined in Scheme 1.

Di(4-bromophenyl)sulfide. Diphenylsulfide (2.34 mL, 20 mmol) was dissolved in a mixed solution of CH_2Cl_2 and H_2O (1:1, 150 mL). Then 30% hydrogen peroxide (0.86 mL, 36 mmol) and bromine (4.1 mL, 80 mmol) were added, and the reaction solution was continuously stirred for 6 h. The resulting mixture was extracted with CH_2Cl_2 with surplus bromine removed by saturated Na_2SO_3 solution. After removing the CH_2Cl_2 solvent, the residue was further purified by silica gel column chromatography (petroleum ether) to give 5.88 g (86%) of a white solid. ^1H NMR (400 MHz, $CDCl_3$) δ [ppm]: 7.45−7.40 (m, 4H), 7.20−7.16 (m, 4H). EI MS (*m*/*z*): 343.86.

Di(4-bromophenyl)sulfone. Di(4-bromophenyl)sulfide (3.44 g, 10 mmol), $KMnO_4$ (5.0 g, 31.6 mmol), and $MnSO_4$ monohydrater (5.0 g, 36.2 mmol) were stirred continuously in CH_2Cl_2 (75 mL) for 10h. After that, the reaction mixture was filtered, and the residue was washed with additional CH_2Cl_2. The crude product was obtained by evaporation of the collected CH_2Cl_2 and was further purified via silica gel column chromatography (CH_2Cl_2/petroleum ether (1:1.5)) to afford 2.3 g (61%) of a white solid. ^1H NMR (400 MHz, $CDCl_3$) δ [ppm]: 7.80−7.76 (m, 4H), 7.67−7.63 (m, 4H). EI MS (*m*/*z*): 373.85.

dx.doi.org/10.1021/cm400945h | *Chem. Mater.* XXXX, XXX, XXX−XXX

*Di(4-(4-(carbazol-9-yl)phenyl)phenyl)sulfone (**CzS1**).* Toluene (6 mL), ethanol (2 mL), and 2 M aqueous Na_2CO_3 (4 mL) were added to a mixture of di(4-bromophenyl)sulfone (374 mg, 1 mmol), 4-(carbazol-9-yl)phenylboronic acid (718 mg, 2.5 mmol), and Pd-$(PPh_3)_4$ (117 mg, 0.1 mmol). With stirring, the suspension was heated at 90 °C for 24 h under a nitrogen atmosphere. When cooled to room temperature, the mixture was extracted with CH_2Cl_2 and dried over Na_2SO_4. After the solvent had been removed, the residue was purified by column chromatography on silica gel (CH_2Cl_2/petroleum ether (2:1)) to give a white solid (532 mg, 76%). ^{1}H NMR (400 MHz, $CDCl_3$) δ [ppm]: 8.15 (t, J = 7.3 Hz, 8H), 7.86−7.80 (m, 8H), 7.71−7.68 (m, 4H), 7.49−7.40 (m, 8H), 7.33−7.29 (m, 4H). ^{13}C NMR is unavailable owing to the poor solubility of the solid. EI MS (m/z): 700.20. Elemental analysis calcd (%) for $C_{48}H_{32}N_2O_2S$: C 82.26, H 4.60, N 4.00, S 4.58; found: C 81.93, H 4.62, N 3.95, S 4.40.

*Di(4-(9-phenylcarbazol-3-yl)phenyl)sulfone (**CzS2**).* The synthetic procedure was similar to that of CzS1, with 4-(carbozol-9-yl)-phenylboronic acid replaced by (9-phenylcarbazol-3-yl)boronic acid, producing a white solid (80%). ^{1}H NMR (400 MHz, $CDCl_3$) δ [ppm]: 8.34 (s, 2H), 8.17 (d, J = 7.7 Hz, 2H), 8.08 (d, J = 8.3 Hz, 4H), 7.84 (d, J = 8.3 Hz, 4H), 7.62−7.55 (m, 10H), 7.50−7.39 (m, 8H), 7.32−7.29 (m, 2H). ^{13}C NMR (100 MHz, $CDCl_3$) δ [ppm]: 147.00, 141.59, 141.13, 139.70, 137.47, 131.31, 130.11, 128.32, 128.02, 127.88, 127.17, 126.62, 125.52, 124.15, 123.34, 120.51, 119.35, 110.45, 110.21. EI MS (m/z): 700.20. Elemental analysis calcd (%) for $C_{48}H_{32}N_2O_2S$: C 82.26, H 4.60, N 4.00, S 4.58; found: C 82.06, H 4.41, N 4.07, S 4.33.

Quantum Calculation. Theoretical calculation of the compounds was carried out using the Gaussian-03 program. Density functional theory (DFT) B3LPY/6-31G(d) was used to determine and optimize the structures. Optimized structures were used for the calculation. No negative mode was found, indicating that the systems indeed correspond to a local energy minimum.

OLED Fabrication and Measurement. ITO coated glass with a sheet resistance of 30 Ω square^{-1} was used as the substrate. Before device fabrication, the ITO glass substrates were cleaned with isopropyl alcohol and deionized water, dried in an oven at 120 °C, treated with UV-ozone, and finally transferred to a vacuum deposition system with a base pressure better than 1×10^{-6} Torr for organic and metal deposition. The devices were fabricated by evaporating organic layers with an evaporation rate of 1−2 Å s^{-1}. The cathode was completed through thermal deposition of LiF at a deposition rate of 0.1 Å s^{-1}, and then capped with Al metal through thermal evaporation at a rate of 10 Å s^{-1}. The overlap between ITO and Al electrodes was 3.3×3.3 mm^2 as the active emissive area of devices. EL luminescence, spectra, and CIE color coordinates were measured with a Spectrascan PR650 photometer, and the current−voltage characteristics were measured with a computer-controlled Keithley 2400 SourceMeter under ambient atmosphere.

RESULTS AND DISCUSSION

Synthesis. CzS1 and CzS2 were similarly prepared through three synthetic steps (Scheme 1) of good yields. Diphenylsulfide was first subjected to the substitution of Br_2.[13] The Br_2 could be rapidly reproduced by H_2O_2 in the two-phase system of CH_2Cl_2/H_2O, which significantly promotes the reaction. The resulting di(4-bromophenyl)sulfide subsequently went through a $MnSO_4$-assisted oxidization by $KMnO_4$,[14] giving the next intermediate di(4-bromophenyl)sulfone. Finally, palladium(0)-catalyzed Suzuki cross-coupling reaction between 4-(carbazol-9-yl)phenylboronic acid/(9-phenylcarbazol-3-yl)-boronic acid and di(4-bromophenyl)sulfone resulted in the target compounds, CzS1/CzS2. These new compounds were characterized with mass spectrometry, ^{1}H NMR, ^{13}C NMR spectroscopy, and elemental analysis.

Thermal Properties. Their good thermal stability was demonstrated by thermogravimetric analysis (TGA), showing high decomposition temperatures T_d (corresponding to 5% weight loss) of 498 °C (CzS1) and 486 °C (CzS2), respectively (Figure 1). High glass transition temperatures (T_g) above 140 °C were also obtained via differential scanning calorimetry (DSC) (Figure 1). Such high T_gs should be attributed to those bulky D-π-A-π-D structures and would benefit the stability of film morphology.

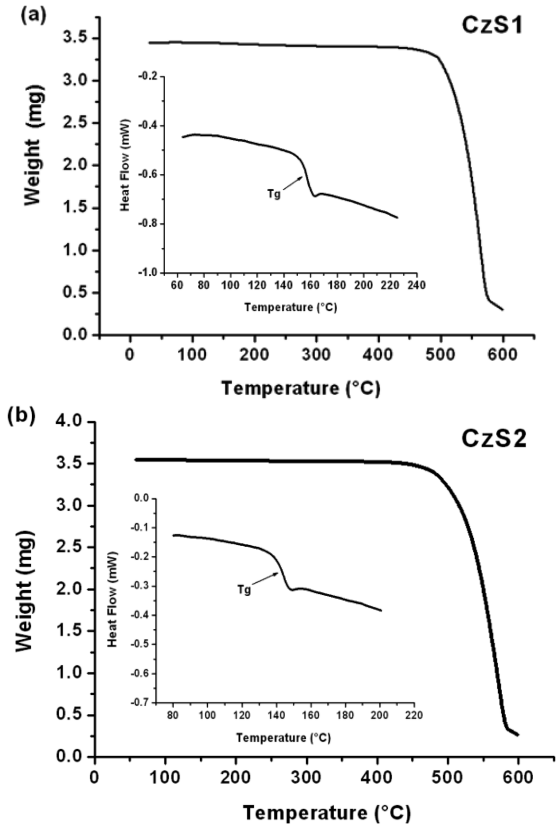

Figure 1. TGA curves (inset: DSC curves) of CzS1 (a) and CzS2 (b).

Optical Properties. Photophysical properties of CzS1 and CzS2 were analyzed using ultraviolet−visible (UV−vis) and photoluminescence (PL) spectrometers. The data are shown in Figure 2, 3 and Table 1. In the absorption spectra of 30 nm thick films, the two compounds show similar absorptions where the bands around 345 and 300 nm can be respectively

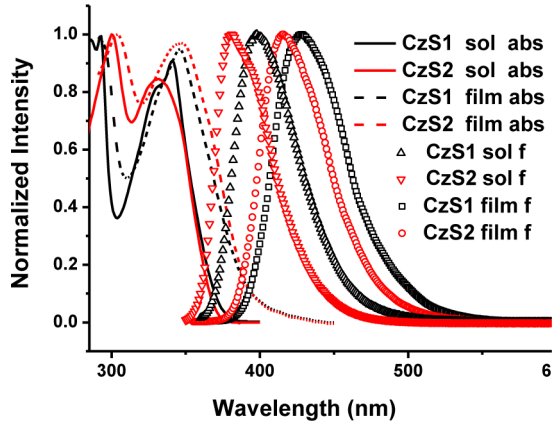

Figure 2. Normalized absorption (lines) and emission (symbols) spectra of CzS1 and CzS2.

dx.doi.org/10.1021/cm400945h | *Chem. Mater.* XXXX, XXX, XXX−XXX

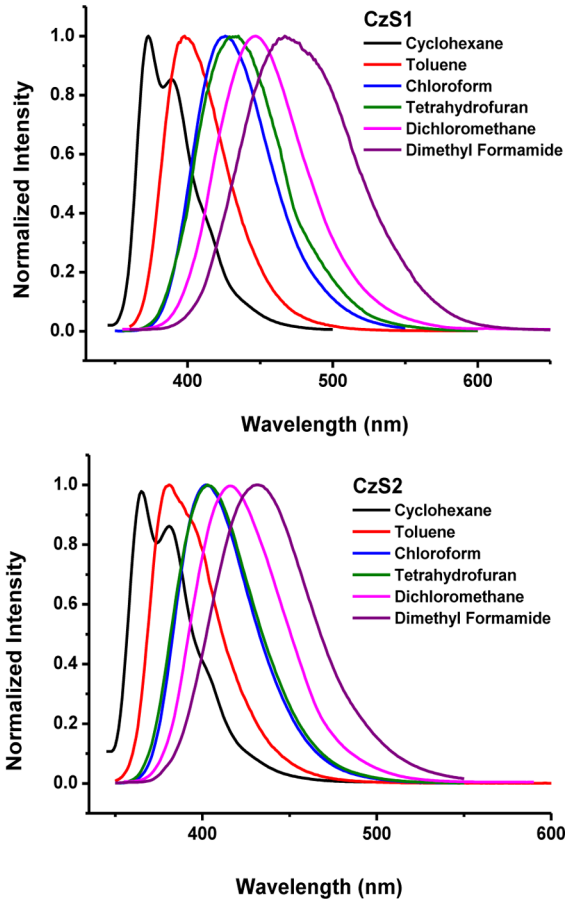

Figure 3. PL spectra of CzS1 (a) and CzS2 (b) in solvents of different polarities.

attributed to the ICT transition and the carbazole-centered n–π^* transition. These absorption bands slightly blue-shift in toluene solution while another distinct shoulder band at 332 nm was found for CzS1. This may arise from the π–π^* transition in the donor units. From the film onset absorptions, both of the band gaps (E_g) of CzS1 and CzS2 are determined to be 3.16 eV. In the film PL spectra, CzS1 exhibits a narrow emission around 428 nm with a fwhm (full width at half-maximum) of 56 nm, while CzS2 shows a relatively blue-shifted emission at 416 nm with a fwhm of 51 nm. Therefore, the film fluorescent emissions of both compounds are located in the short-wavelength spectral region of the whole visible light spectrum. To illustrate the reasonable molecular design in this work, we may also compare their solution PL characteristics with compound **11**, namely, 2,8-di(*N*-(2-ethylhexyl)-carbazol-3-yl) dibenzothiophene-S,S-dioxide, which has the highest-energy fluorescence of 408 nm in toluene among its carbazole/DBTO analogues reported by Moss et al.[11] In our case, both of the new compounds give violet fluorescence with maximum wavelengths below 400 nm in the same solution. The higher energy fluorescence of our compounds should be primarily ascribed to the reasonable molecular design using conjugation-limited diphenylsulfone block instead of the planar DBTO unit. The ICT characteristics of the two emitters are shown via their gradually red-shifted and broadened fluorescent emissions upon increasing the polarity of solvent (Figure 3). Large increase of the dipole moment from the ground state to the excited state was also calculated from the Lippert–Mataga calculation, 37 D for CzS1 and 24 D for CzS2 (see Supporting Information),[15] further reflecting the typical photoinduced ICT process and the effective electronic communication between the donor and acceptor units. In addition, fluorescent quantum yields of CzS1 and CzS2 were estimated to be approaching unity in toluene, as referenced to quinine sulfate (Φ_f = 0.56 in 1 N H_2SO_4).[16] Such high quantum yields (four times over that of compound **11**, 0.25) are owing to the suitably modified D-π-A molecular structures which could provide highly emissive ICT excited states upon excitation. Even in neat films, these yields still remain impressively high as measured by the integrating sphere method under air condition, 0.98 for CzS1 and 0.79 for CzS2, suggesting that the fluorescence quenching routes in the film have been effectively suppressed, probably owing to the bulky D-π-A-π-D structures.

Adachi and co-workers have recently made a milestone advance in the organic electroluminescence research field by introducing purely organic molecules that can give efficient thermally activated delayed fluorescence (TADF) through up-conversion of triplet to singlet states, and therefore lead to potentially 100% internal singlet yields.[10h,17] Among their reported TADF materials, compound **3**, namely, di(4-(3,6-di-*tert*-butylcarbazol-9-yl)phenyl)sulfone, shows pure-blue electroluminescence with extremely high EQE of 9.9%.[10h] Considering that the two compounds in this work have similar molecular structures with compound **3**, we also explore their potential of TADF emission. Supporting Information, Figure S2 shows their room-temperature transient PL decay characteristics in an oxygen-free toluene solution. The samples were freshly nitrogen-purged to avoid any possible triplet quenching by oxygen. It is interesting to find that, in contrast to the case of compound **3** in the report of Adachi et al., both of our new compounds clearly exhibit first-order exponential decays which completely end within a short time range of 20 ns. Indeed, no delayed components were observed in both cases, indicating the absence of DATF emission from CzS1 and CzS2. We may mainly attribute this to the overwhelming emission transition rate over the nonemission transition rate of their photoinduced excited states. As mentioned above, CzS1 and CzS2 achieved near-unity fluorescent quantum yields even in the air-equilibrated toluene solution, and therefore one can deduce that the intersystem crossing (ISC) process, one non-emission

Table 1. Physical Properties of These Novel Fluorophores

	λ_{abs},[a] (nm) (log ε)[b]	λ_f[a] (nm)	λ_{abs}[c] (nm)	λ_f[c] (nm)	E_g[d] (eV)	τ[e] (ns)	Φ_f[a,c]	ΔE_{ST}[f] (eV)	T_g/T_d (°C)	E_{ox}[g] (V)	HOMO (eV)	LUMO (eV)
CzS1	293(4.51), 332(4.42), 341(4.47)	399	293, 346	428	3.16	2.55	~1 (0.98)	0.62	157/498	0.81	−5.61	−2.45
CzS2	300(4,81), 332(4.73)	381, 392	304, 347	416	3.16	1.51	~1 (0.79)	0.65	143/486	0.82	−5.62	−2.46

[a]Measured in an air-equilibrated toluene solution. [b]ε is the extinction coefficient (in M^{-1} cm^{-1}). [c]Measured in 30 nm-thick film state. [d]Energy band gap as determined from the film absorption edge. [e]Lifetime of the fluorescence as determined in an oxygen-free toluene solution. [f]Estimated from the low-temperature fluorescence and phosphorescence maxima. [g]The onset potential of oxidation as referenced to ferrocene (Fc).

dx.doi.org/10.1021/cm400945h | *Chem. Mater.* XXXX, XXX, XXX–XXX

route which is supposed to create a triplet state, is significantly suppressed. On the other hand, as delayed fluorescence is established by the premise of converting the triplet back to a singlet state, the energy distance (ΔE_{ST}) between the lowest singlet state and the lowest triplet state should be taken into account; generally, the smaller ΔE_{ST} the more efficient the up-conversion. Estimated from the low-temperature fluorescence and phosphorescence maxima, we obtained the ΔE_{ST} of 0.62 and 0.65 eV respectively for CzS1 and CzS2 (see Supporting Information, Figure S3). As a result, these compounds show much larger ΔE_{ST} than the reported 0.32 eV for compound **3**, which should dramatically raise the difficulty of up-converting triplet to singlet state to give delayed fluorescence.

Electrochemical Properties. Cyclic voltammetry (CV) was conducted to measure the HOMO levels of CzS1 and CzS2. From the onset of the oxidation curves (Figure 4), the highest occupied molecular orbital (HOMO) levels were estimated to be −5.61 and −5.62 eV for CzS1 and CzS2, respectively, by comparing with ferrocene (Fc) (HOMO = $-(E_{ox} + 4.8)$ eV).[18] Their LUMO levels were further estimated by summing the HOMO levels and the band gaps determined from their absorption edges. These orbital energy levels are listed in Table 1. The similarity of molecular orbital energy levels should be associated with the fact that these molecules incorporate identical functional groups and similar D-π-A structures. To gain insight into the electronic structures of these compounds, a density functional theory (DFT) calculation was performed at the B3LYP/6-31G (d) level. Figure 5 reveals an obvious separation of the HOMO and the LUMO which are dominantly located on the carbazole and the diphenylsulfone units respectively. This separation should effectively maintain the individual electronic properties of these functional groups and benefit the transport of both holes and electrons.[19] In addition, it can also be observed that there are still enough HOMO−LUMO overlaps. These are required to guarantee effective electronic communication between the donor and the acceptor, and thus highly emissive ICT excited states which have already been demonstrated by the high fluorescent quantum yields.[20]

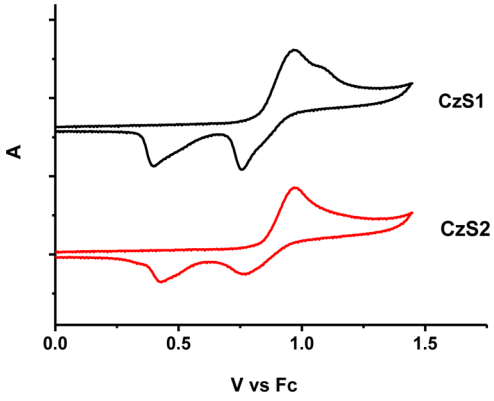

Figure 4. Cyclic voltammograms of CzS1 and CzS2 in CH_2Cl_2.

Electroluminescence. To investigate the EL performance of CzS1 and CzS2, two nondoped fluorescent OLEDs were fabricated with a configuration of ITO/NPB (30 nm)/mCP (10 nm)/ CzS1 or CzS2 (30 nm)/TPBI (30 nm)/LiF (1.5 nm)/Al (100 nm). Figure 6 shows the EL spectra of the devices

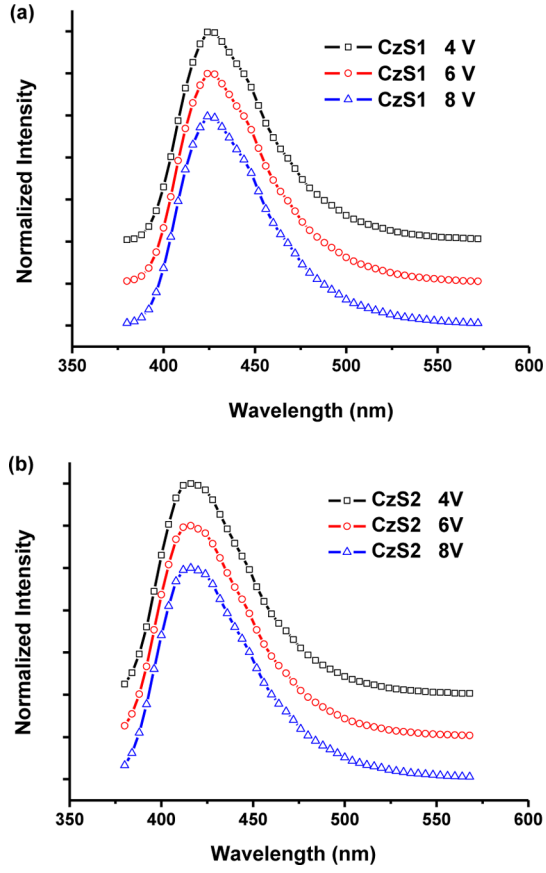

Figure 6. EL spectra of the CzS1 (a) and the CzS2 (b) based devices at different voltages.

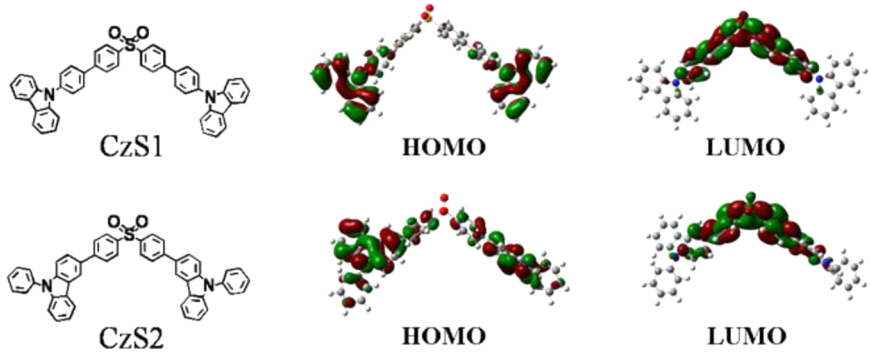

Figure 5. Simulated electronic distributions of CzS1 and CzS2's HOMOs and LUMOs.

dx.doi.org/10.1021/cm400945h | *Chem. Mater.* XXXX, XXX, XXX−XXX

at different driving voltages. The EL spectra are almost identical to the corresponding PL spectra of their neat films and show little change under different driving voltages. These spectral characteristics imply a good confinement of excitons in the emission layers, which are attributed to the wide band gaps of the adjacent mCP (3.5 eV) and TPBI (3.4 eV) (Figure 7).[21]

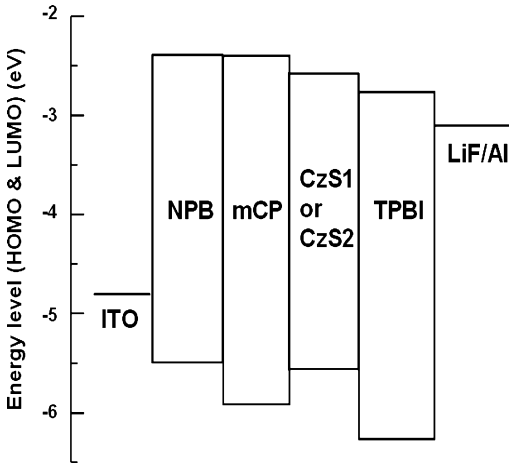

Figure 7. Energy level diagram of the devices.

CIE coordinates of (0.157, 0.055) and (0.157, 0.044) were respectively observed for the CzS1 and the CzS2 devices at brightness of 100 cd m^{-2}. According to the CIE chromaticity diagram, CzS1 and CzS2 show intrinsic blue-violet electroluminescence in these nondoped devices. Performances of these devices are further shown in Figure 8 and Table 2. From the current density−voltage−luminescence (*J-V-L*) plots, it can be observed that CzS2 device achieved an extremely low turn-on voltage of 2.8 V, as well as much higher current densities under the same voltage as compared to the CzS1 device. These might be owing to the better charge-transporting ability of CzS2. However, the CzS2-based device exhibits relatively lower efficiencies with maximum EQE of 2.7%, CE of 0.82 cd A^{-1}, and PE of 0.84 lm W^{-1}, while the device based on CzS1 presents impressive EL performance with high maximum EQE, CE, and PE of 4.2%, 1.89 cd A^{-1} and 1.58 lm W^{-1}, respectively. The CE and PE in this work currently have represented the best results for OLEDs with CIE_y < 0.06 (Table 2).[4] Even at the practical luminescence of 1000 cd m^{-2}, the EQE and CE of the CzS1 device still remain high as 3.2% and 1.45 cd A^{-1}, indicative of a relatively low efficiency roll-off.

Single-Carrier Devices. To understand the different EL performance as well as to demonstrate the bipolar properties of these fluorophores, hole-only and electron-only devices of CzS1 and CzS2 were fabricated. The configuration of the hole-only device is ITO/NPB (30 nm)/mCP (10 nm)/ CzS1 or CzS2 (30 nm)/MoO_3 (10 nm)/Al (100 nm), and the electron-only device have the structure of ITO/TPBI (20 nm)/ CzS1 or CzS2 (30 nm)/TPBI (30 nm)/LiF (1.5 nm)/Al (100 nm). MoO_3 in the first configuration (LUMO = −2.3 eV) and TPBI (20 nm) in the second configuration (HOMO = −6.2 eV) were respectively utilized to block the electron-injection from Al (−4.3 eV, corresponding to a large energy barrier of 2.0 eV) and the hole-injection from ITO (−4.8 eV, corresponding to a large energy barrier of 1.4 eV).[22] Moreover, the other parts for charge injection/transport were kept unchanged from these blue-violet light-emitting devices. As shown in Figure 9, all the

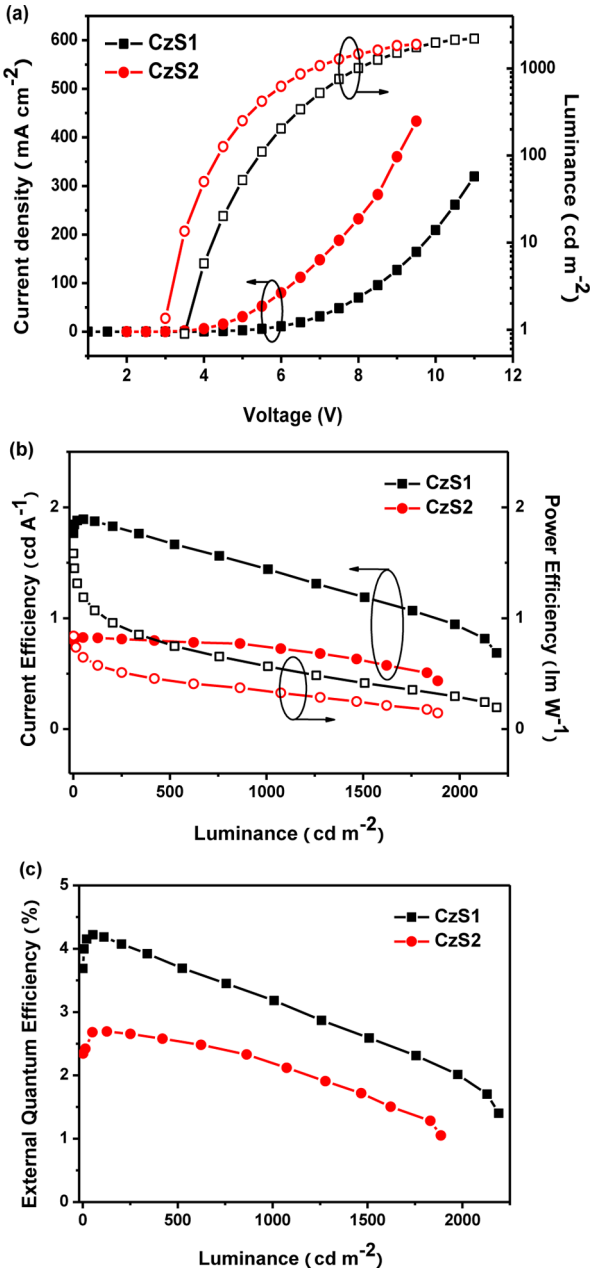

Figure 8. (a) Current density−voltage−luminance characteristics, (b) current efficiency−luminance−power efficiency plots, and (c) external quantum efficiency−luminance plots of the CzS1 and the CzS2 based blue-violet light-emitting devices.

four single-carrier devices show significant currents, indicating the bipolar charge-transporting abilities of both CzS1 and CzS2. Additionally, it is also found that the hole and electron currents of the CzS2 devices are both much higher, however, less balanced as compared to those of the CzS1 devices. These could explain why the light-emitting device based on CzS2 achieved relatively lower turn-on voltage and higher current density/luminescence while the CzS1-based device achieved higher EL efficiencies. It is thus reflected that charge balance is an important factor for the device efficiencies.[23]

CONCLUSIONS

In summary, two highly efficient blue-violet fluorophores, CzS1 and CzS2, have been developed via a D-π-A structure design

dx.doi.org/10.1021/cm400945h | *Chem. Mater.* XXXX, XXX, XXX−XXX

Table 2. Key Characteristics Summary of the CzS1 and the CzS2-Based Devices and Other High Performance Blue-Violet/Violet Light-Emitting Devices with $CIE_y \leq 0.06$

emitters	V_{on} [V]	CE[a] [cd A^{-1}]	PE[b] [lm W^{-1}]	EQE[c] [%]	$\lambda_{f,max}$[d] [nm]	CIE	ref
CzS1	3.5	1.89/1.88/1.45	1.58/1.10/0.57	4.21/4.20/3.19	426	(0.157,0.055)	this work[e]
CzS2	2.8	0.82/0.82/0.73	0.84/0.59/0.33	2.7/2.69/2.2	417	(0.157,0.044)	this work[e]
TDAF1	2.5	1.53/ -/ -	-/ -/ -	5.3/ -/ -		(0.158, 0.041)	4a[e]
TDAF2	2.5	1.1/ -/ -	-/ -/ -	4.1/ -/ -		(0.160, 0.044)	4a[e]
CPhBzIm	2.5	1.6/ -/ -	1.07/ -/ -	3/ -/ 2.4	426	(0.16, 0.05)	4d[e]
Cz-2pbb	2.5−3	-/ -/ -	-/ -/ -	4.1/ -/ -	410	(0.16, 0.05)	4e[f]
M1		0.65/ -/ -	0.48/ -/ -	1.94/ -/ -	420	(0.165, 0.050)	4g[e]
M2		1.53/ -/ -	0.86/ -/ -	3.02/ -/ -	428	(0.166, 0.056)	4g[e]
TPA(3)-F		0.39/ -/ -	-/ -/ -	-/ -/ -	428	(0.16, 0.06)	4f[e]
TCPC-4		0.9/ -/ -	-/ -/ -	2.47/ -/ -	425	(0.16, 0.05)	4h[e]
TCPC-6		1.35/ -/ -	-/ -/ -	3.72/ -/ -	425	(0.16, 0.05)	4h[e]
Purine 1	2.9	-/ -/ -	-/ -/ -	3.1/ -/ -	432	(0.15, 0.06)	4i[f]
Purine 2	3.2	-/ -/ -	-/ -/ -	1.6/ -/ -	393		4j[f]

[a]Current efficiency. [b]Power efficiency. [c]External quantum efficiency respectively corresponding to the maximum value, the value at brightness of 100 cd m^{-2} and 1000 cd m^{-2}. [d]The maximum electroluminescence wavelength. [e]Nondoped. [f]Doped devices.

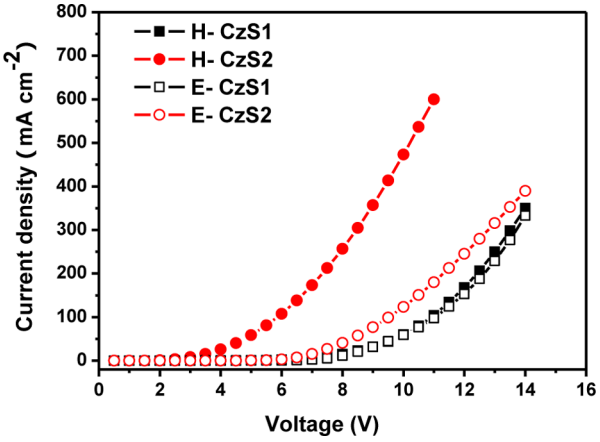

Figure 9. Current density−voltage curves of the CzS1- and the CzS2-based hole-only and electron-only devices.

strategy which incorporates carbazole as a mild electron-donor and sulfone as an electron-acceptor with a π-conjugation-breaking feature. Nondoped devices based on the two compounds exhibit blue-violet light emissions with CIE coordinates of (0.157, 0.055) for CzS1 and (0.157, 0.044) for CzS2 at 100 cd m^{-2}, respectively. CzS1 possesses much better balanced bipolar charge-transporting ability, and its electroluminescence device shows high performance with EQE, CE, and PE of 4.2%, 1.89 cd A^{-1}, and 1.58 lm W^{-1}, respectively, which are among the best of blue-violet/violet OLEDs up until now. We here successfully provide an efficient design strategy for high-efficiency short-wavelength fluorophores.

■ ASSOCIATED CONTENT

Supporting Information

Lippert−Mataga calculation, molecular orbital quantum calculation, emission decay in toluene, and low-temperature luminescence and phosphorescence. This material is available free of charge via the Internet at http://pubs.acs.org.

■ AUTHOR INFORMATION

Corresponding Author

*E- mail: xhzhang@mail.ipc.ac.cn (X.Z.), apcslee@cityu.edu.hk (C.-S.L.).

Author Contributions

[‖]J.Y. and Z.C. contributed equally to this work.

Notes

The authors declare no competing financial interest.

■ ACKNOWLEDGMENTS

The authors are grateful to the National Natural Science Foundation of China (Grants 50825304,51033007, 51103169, 51128301) and Beijing Natural Science Foundation (Grant 2111002), P. R. China. Prof. C. S. Lee would like to acknowledge support from the Research Grants Council of the Hong Kong (Project No. T23-713/11).

■ REFERENCES

(1) (a) Kraft, A.; Grimsdale, A. C.; Holmes, A. B. *Angew. Chem., Int. Ed.* **1998**, *37*, 402. (b) O'Brien, D. F.; Baldo, M. A.; Thompson, M. E.; Forrest, S. R. *Appl. Phys. Lett.* **1999**, *74*, 442. (c) Chao, T. C.; Lin, Y. T.; Yang, C. Y.; Hung, T. S.; Chou, H. C.; Wu, C. C.; Wong, K. T. *Adv. Mater.* **2005**, *17*, 992. (d) Li, H. Y.; Batsanov, A. S.; Moss, K. C.; Vaughan, H. L.; Dias, F. B.; Kamtekar, K. T.; Bryce, M. R.; Monkman, A. P. *Chem. Commun.* **2010**, *46*, 4812.

(2) Santen, H. v.; Neijzen, J. H. M. *Jpn. J. Appl. Phys., Part 1* **2003**, *42*, 1110.

(3) Tung, Y. J.; Nago, T.; Hack, M.; Brown, J.; Koide, N.; Nagara, Y.; Kato, Y.; Ito, a. H. *Dig. Tech. Pap. - Soc. Inf. Disp. Int. Symp.* **2004**, *35*, 48.

(4) (a) Wu, C. C.; Lin, Y. T.; Wong, K. T.; Chen, R. T.; Chien, Y. Y.. *Adv. Mater.* **2004**, *16*, 61. (b) Huang, F.; Niu, Y. H.; Liu, M. S.; Zhou, X. H.; Tian, Y. Q.; Jen, A. K. Y. *Appl. Phys. Lett.* **2006**, 89. (c) Zhou, X. H.; Niu, Y. H.; Huang, F.; Liu, M. S.; Jen, A. K. Y. *Macromolecules* **2007**, *40*, 3015. (d) Hung, W. Y.; Chi, L. C.; Chen, W. J.; Chen, Y. M.; Chou, S. H.; Wong, K. T. *J. Mater. Chem.* **2010**, *20*, 10113. (e) Yang, X. H.; Zheng, S. J.; Bottger, R.; Chae, H. S.; Tanaka, T.; Li, S.; Mochizuki, A.; Jabbour, G. E. *J. Phys. Chem. C* **2011**, *115*, 14347. (f) Li, Z. F.; Wu, Z. X.; Fu, W.; Liu, P.; Jiao, B.; Wang, D. D.; Zhou, G. J.; Hou, X. *J. Phys. Chem. C* **2012**, *116*, 20504. (g) Gao, Z.; Liu, Y.; Wang, Z.; Shen, F.; Liu, H.; Sun, G.; Yao, L.; Lv, Y.; Lu, P.; Ma, Y. *Chem.—Eur. J.* **2013**, *19*, 2602. (h) Tang, S.; Liu, M.; Lu, P.; Xia, H.; Li, M.; Xie, Z. Q.; Shen, T. Z.; Gu, C.; Wang, H. P.; Yang, B.; Ma, Y. G. *Adv. Funct. Mater.* **2007**, *17*, 2869. (i) Yang, Y. X.; Cohn, P.; Dyer, A. L.; Eom, S. H.; Reynolds, J. R.; Castellano, R. K.; Xue, J. G. *Chem. Mater.* **2010**, *22*, 3580. (j) Yang, Y. X.; Cohn, P.; Eom, S. H.; Abboud, K. A.; Castellano, R. K.; Xue, J. G. *J. Mater. Chem.* **2013**, *1*, 2867.

(5) (a) Adachi, C.; Tsutsui, T.; Saito, S. *Appl. Phys. Lett.* **1990**, *56*, 799. (b) Kim, Y. H.; Jeong, H. C.; Kim, S. H.; Yang, K. Y.; Kwon, S. K. *Adv. Funct. Mater.* **2005**, *15*, 1799. (c) Kim, S. K.; Yang, B.; Ma, Y.;

Lee, J. H.; Park, J. W. *J. Mater. Chem.* **2008**, *18*, 3376. (d) Tao, S.; Zhou, Y. C.; Lee, C. S.; Lee, S. T.; Huang, D.; Zhang, X. H. *J. Phys. Chem. C* **2008**, *112*, 14603. (e) Wu, C. H.; Chien, C. H.; Hsu, F. M.; Shih, P. I.; Shu, C. F. *J. Mater. Chem.* **2009**, *19*, 1464. (f) Kim, S. K.; Yang, B.; Park, Y. I.; Ma, Y. G.; Lee, J. Y.; Kim, H. J.; Park, J. *Org. Electron.* **2009**, *10*, 822. (g) Zheng, C. J.; Zhao, W. M.; Wang, Z. Q.; Huang, D.; Ye, J.; Ou, X. M.; Zhang, X. H.; Lee, C. S.; Lee, S. T. *J. Mater. Chem.* **2010**, *20*, 1560.

(6) (a) Lee, S. H.; Tsutsui, T. *Thin Solid Films* **2000**, *363* (1−2), 76−80. (b) Tao, S. L.; Peng, Z. K.; Zhang, X. H.; Wang, P. F.; Lee, C. S.; Lee, S. T. *Adv. Funct. Mater.* **2005**, *15*, 1716. (c) Zhen, C. G.; Chen, Z. K.; Liu, Q. D.; Dai, Y. F.; Shin, R. Y. C.; Chang, S. Y.; Kieffer, J. *Adv. Mater.* **2009**, *21*, 2425. (d) Ku, S. Y.; Chi, L. C.; Hung, W. Y.; Yang, S. W.; Tsai, T. C.; Wong, K. T.; Chen, Y. H.; Wu, C. I. *J. Mater. Chem.* **2009**, *19*, 773. (e) Matsumoto, N.; Miyazaki, T.; Nishiyama, M.; Adachi, C. *J. Phys. Chem. C* **2009**, *113*, 6261. (f) Wang, S. A.; Hung, W. Y.; Chen, Y. H.; Wong, K. T. *Org. Electron.* **2012**, *13*, 1576.

(7) (a) Hosokawa, C.; Higashi, H.; Nakamura, H.; Kusumoto, T. *Appl. Phys. Lett.* **1995**, *67*, 3853. (b) Lee, M. T.; Liao, C. H.; Tsai, C. H.; Chen, C. H. *Adv. Mater.* **2005**, *17*, 2493. (c) Chou, H. H.; Chen, Y. H.; Hsu, H. P.; Chang, W. H.; Cheng, C. H. *Adv. Mater.* **2012**, *24*, 5867.

(8) (a) Yang, C. H.; Guo, T. F.; Sun, I. W. *J. Lumin.* **2007**, *124*, 93. (b) Qin, T. S.; Wiedemair, W.; Nau, S.; Trattnig, R.; Sax, S.; Winkler, S.; Vollmer, A.; Koch, N.; Baumgarten, M.; List, E. J. W.; Mullen, K. *J. Am. Chem. Soc.* **2011**, *133*, 1301. (c) Zhao, Z. J.; Ye, S. H.; Guo, Y. J.; Chang, Z. F.; Lin, L. Y.; Jiang, T.; Lam, J. W. Y.; Lu, P.; Qiu, H. Y.; Liu, Y. Q.; Tang, B. Z. *Org. Electron.* **2011**, *12*, 2236. (d) Wang, Z. Q.; Xu, C.; Wang, W. Z.; Dong, X. M.; Zhao, B. T.; Ji, B. M. *Dyes Pigments* **2012**, *92*, 732.

(9) (a) Kulkarni, A. P.; Tonzola, C. J.; Babel, A.; Jenekhe, S. A. *Chem. Mater.* **2004**, 4556. (b) Shirota, Y.; Kageyama, H. *Chem. Rev.* **2007**, *107*, 953.

(10) (a) Huang, T. H.; Lin, J. T.; Chen, L. Y.; Lin, Y. T.; Wu, C. C. *Adv. Mater.* **2006**, *18*, 602. (b) Lee, S. J.; Park, J. S.; Yoon, K. J.; Kim, Y. I.; Jin, S. H.; Kang, S. K.; Gal, Y. S.; Kang, S.; Lee, J. Y.; Kang, J. W.; Lee, S. H.; Park, H. D.; Kim, J. J. *Adv. Funct. Mater.* **2008**, *18*, 3922. (c) Lin, S. L.; Chan, L. H.; Lee, R. H.; Yen, M. Y.; Kuo, W. J.; Chen, C. T.; Jeng, R. J. *Adv. Mater.* **2008**, *20*, 3947. (d) Lai, M. Y.; Chen, C. H.; Huang, W. S.; Lin, J. T.; Ke, T. H.; Chen, L. Y.; Tsai, M. H.; Wu, C. C. *Angew. Chem., Int. Ed.* **2008**, *47*, 581. (e) Chen, C. H.; Huang, W. S.; Lai, M. Y.; Tsao, W. C.; Lin, J. T.; Wu, Y. H.; Ke, T. H.; Chen, L. Y.; Wu, C. C. *Adv. Funct. Mater.* **2009**, *19*, 2661. (f) Zhang, Y.; Lai, S. L.; Tong, Q. X.; Lo, M. F.; Ng, T. W.; Chan, M. Y.; Wen, Z. C.; He, J.; Jeff, K. S.; Tang, X. L.; Liu, W. M.; Ko, C. C.; Wang, P. F.; Lee, C. S. *Chem. Mater.* **2012**, *24*, 61. (g) Linton, K. E.; Fisher, A. L.; Pearson, C.; Fox, M. A.; Palsson, L. O.; Bryce, M. R.; Petty, M. C. *J. Mater. Chem.* **2012**, *22*, 11816. (h) Zhang, Q. S.; Li, J.; Shizu, K.; Huang, S. P.; Hirata, S.; Miyazaki, H.; Adachi, C. *J. Am. Chem. Soc.* **2012**, *134*, 14706. (i) Nakagawa, T.; Ku, S. Y.; Wong, K. T.; Adachi, C. *Chem. Commun.* **2012**, *48*, 9580. (j) Liu, C.; Gu, Y.; Fu, Q.; Sun, N.; Zhong, C.; Ma, D. G.; Qin, J. G.; Yang, C. L. *Chem.—Eur. J.* **2012**, *18*, 13828.

(11) Moss, K. C.; Bourdakos, K. N.; Bhalla, V.; Kamtekar, K. T.; Bryce, M. R.; Fox, M. A.; Vaughan, H. L.; Dias, F. B.; Monkman, A. P. *J. Org. Chem.* **2010**, *75*, 6771.

(12) Sasabe, H.; Seino, Y.; Kimura, M.; Kido, J. *Chem. Mater.* **2012**, *24*, 1404.

(13) Bravo, A.; Dordi, B.; Fontana, F.; Minisci, F. *J. Org. Chem.* **2001**, *66*, 3232.

(14) Shaabani, A.; Rahmati, A.; Sharifi, M.; Rad, J. M.; Aghaaliakbari, B.; Farhangi, E.; Lee, D. G. *Monatsh. Chem.* **2007**, *138*, 649.

(15) (a) Lippert, E. *Z. Naturforsch.* **1955**, *10*, 541. (b) Mataga, N.; Kaifu, Y.; Koizumi, M. *Bull. Chem. Soc. Jpn.* **1955**, *28*, 69. (c) Mataga, N.; Kubota, T. *Molecular Interactions and Electronic Spectra*; Marcel Dekker: New York, 1970.

(16) Eaton, D. F. *Pure Appl. Chem.* **1988**, *60*, 1107.

(17) (a) Uoyama, H.; Goushi, K.; Shizu, K.; Nomura, H.; Adachi, C. *Nature* **2012**, *492*, 234. (b) Goushi, K.; Yoshida, K.; Sato, K.; Adachi, C. *Nat. Photonics* **2012**, *6*, 253. (c) Mehes, G.; Nomura, H.; Zhang, Q. S.; Nakagawa, T.; Adachi, C. *Angew. Chem., Int. Ed.* **2012**, *51*, 11311.

(18) Pommerehne, J.; Vestweber, H.; Guss, W.; Mahrt, R. F.; Bassler, H.; Porsch, M.; Daub, J. *Adv. Mater.* **1995**, *7*, 551.

(19) Zheng, C. J.; Ye, J.; Lo, M. F.; Fung, M. K.; Ou, X. M.; Zhang, X. H.; Lee, C. S. *Chem. Mater.* **2012**, *24*, 643.

(20) Schwartz, G.; Reineke, S.; Rosenow, T. C.; Walzer, K.; Leo, K. *Adv. Funct. Mater.* **2009**, *19*, 1319.

(21) Liu, H.; Cheng, G.; Hu, D. H.; Shen, F. Z.; Lv, Y.; Sun, G. N.; Yang, B.; Lu, P.; Ma, Y. G. *Adv. Funct. Mater.* **2012**, *22*, 2830.

(22) Wang, K.; Zhao, F. C.; Wang, C. G.; Chen, S. Y.; Chen, D.; Zhang, H. Y.; Liu, Y.; Ma, D. G.; Wang, Y. *Adv. Funct. Mater.* **2013**, *23*, 2672.

(23) (a) Pu, Y. J.; Nakata, G.; Satoh, F.; Sasabe, H.; Yokoyama, D.; Kido, J. *Adv. Mater.* **2012**, *24*, 1765. (b) Chopra, N.; Lee, J.; Zheng, Y.; Eom, S. H.; Xue, J. E.; So, F. *ACS Appl. Mater. Interfaces.* **2009**, *1*, 1169.